

GRACE terrestrial water storage data assimilation based on the ensemble four-dimensional variational method PODEn4DVar: Method and validation

SUN Qin^{1,2,3}, XIE ZhengHui^{1*} & TIAN XiangJun¹

¹ State Key Laboratory of Numerical Modelling for Atmospheric Sciences and Geophysical Fluid Dynamics (LASG),
Institute of Atmospheric Physics, Chinese Academy of Sciences, Beijing 100029, China;

² University of Chinese Academy of Sciences, Beijing 100049, China;

³ Numerical Weather Prediction Center, China Meteorological Administration, Beijing 100081, China

Received February 10, 2014; accepted August 26, 2014

Seasonal and interannual changes in the Earth's gravity field are mainly due to mass exchange among the atmosphere, ocean, and continental water sources. The terrestrial water storage changes, detected as gravity changes by the Gravity Recovery and Climate Experiment (GRACE) satellites, are mainly caused by precipitation, evapotranspiration, river transportation and downward infiltration processes. In this study, a land data assimilation system LDAS-G was developed to assimilate the GRACE terrestrial water storage (TWS) data into the Community Land Model (CLM3.5) using the POD-based ensemble four-dimensional variational assimilation method PODEn4DVar, disaggregating the GRACE large-scale terrestrial water storage changes vertically and in time, and placing constraints on the simulation of vertical hydrological variables to improve land surface hydrological simulations. The ideal experiments conducted at a single point and assimilation experiments carried out over China by the LDAS-G data assimilation system showed that the system developed in this study improved the simulation of land surface hydrological variables, indicating the potential of GRACE data assimilation in large-scale land surface hydrological research and applications.

data assimilation, land surface model, terrestrial water storage, ensemble four-dimensional variational data assimilation method

Citation: Sun Q, Xie Z H, Tian X J, et al. 2015. GRACE terrestrial water storage data assimilation based on the ensemble four-dimensional variational method PODEn4DVar: Method and validation. *Science China: Earth Sciences*, 58: 371–384, doi: 10.1007/s11430-014-4978-1

Changes in the Earth's gravity field reflect the redistribution of the Earth's mass, and thus the migration and exchange of the Earth's mass can be estimated from gravity observations (Sun, 2002). Seasonal and interannual gravitational changes are mainly caused by mass exchange among the atmosphere, ocean and continental water sources through the processes of precipitation, river transportation, evaporation, and melting of glaciers and the Arctic ice cap (Tapley et al., 2004a; Hu et al., 2006). Changes in terrestrial water storage (main-

ly due to precipitation, evapotranspiration, river transportation and downward infiltration processes) are also reflected in gravity observations. Changes of each component of the water cycle can therefore be assessed and applied in water resource management and water cycle research.

The Gravity Recovery and Climate Experiment (GRACE) gravity observation satellites were launched in 2002 as a joint National Aeronautics and Space Administration (NASA) and German Aerospace Center (Deutsche Luftfahrtmitte, DLR) project (Tapley et al., 2004b) to detect gravity anomalies and estimate large-scale changes of column-integrated terrestrial water storage (TWS) for the en-

*Corresponding author (email: zxie@lasg.iap.ac.cn)

tire globe, providing valuable information for regional and continental scale hydrological research. The GRACE measurements have been applied in novel investigations of global and regional terrestrial water storage changes (Syed et al., 2008; Zhong et al., 2009; Grippa et al., 2011; Su et al., 2012; Xu et al., 2013), terrestrial water budget (Sheffield et al., 2009; Troy et al., 2011), terrestrial freshwater discharge (Syed et al., 2009), sea level variations (Konikow, 2011; Llovel et al., 2011; Wouters et al., 2011), the changing mass of ice sheets (Chen et al., 2009a; Chen et al., 2011), drought events (Chen et al., 2009b, 2010), regional evapotranspiration (Rodell et al., 2004), parameter improvement for water table depth (WTD) simulation (Lo et al., 2010), and model evaluations (Niu and Yang 2006a, Niu et al., 2007b), all of which have yielded important insights into the land surface water cycle at regional and global scales.

Estimates of terrestrial water storage anomalies (TWSA) using GRACE observations are generated monthly, with a spatial resolution limited to about 150000 km² (Rowlands et al., 2005). Vertically, GRACE TWSA observations integrate changes in groundwater (GW), soil moisture (SM), surface water, vegetation water, snow and ice. In order to realize the full potential of GRACE to improve the simulations of these components, the monthly and column-integrated TWSA data must be disaggregated vertically and in time (Zaitchik et al., 2008). Rodell et al. (2007) estimated regional groundwater storage (GWS) variations by removing the modeled SM and snow water equivalent (SWE) from GRACE data, assuming that the contributions of vegetation and surface water were negligible. Yeh et al. (2006) used SM observations to isolate GWS variations from GRACE TWSA. Niu et al. (2007a) derived the SWE for basins in Arctic regions from GRACE TWSA data with the aid of modeled below-ground water storage, to compensate for the large errors that occurred in the measurements by microwave sensors in regions of boreal forest and deep snow. Feng et al. (2013) estimated GWS variations by removing simulated SM from GRACE TWSA, and discussed groundwater depletion in North China. These studies, which evaluated variations in components of the water cycle using GRACE measurements, all isolated individual components from GRACE TWSA with the aid of auxiliary information.

Another more sophisticated method is to merge GRACE-derived TWSA information into a land surface model (LSM) via data assimilation, and thus achieve vertical disaggregation through the dynamic framework of the model. For example, Zaitchik et al. (2008) assimilated GRACE TWSA information into an LSM using an ensemble Kalman smoother (EnKS) in the Mississippi River Basin, and improved simulations of hydrological variable variations on a smaller scale than the GRACE observations themselves, indicating that data assimilation had the potential to downscale the GRACE data for hydrological applications. Su et al. (2010) investigated the effect of GRACE

data assimilation on snowpack estimation by assimilating both GRACE TWSA information and MODIS snow cover fraction information. Forman et al. (2012) applied GRACE data assimilation for a snow-dominated basin in northwest Canada. Houborg et al. (2012) and Li et al. (2012) applied GRACE data assimilation for drought monitoring in North America and Europe respectively. These studies calculated assimilation increments monthly and update on a daily scale, and all used the EnKS method for GRACE data assimilation.

To assign assimilation increments on a more natural basis, in the present study, GRACE data assimilation was carried out by an ensemble variational assimilation method. Many developments have recently been reported on assimilation methods and systems and their applications for land, atmosphere and ocean research (Zhu et al., 2007; Wang and Mu, 2008; Li et al., 2007; Qiu et al., 2007; Yang et al., 2007; Wang et al., 2010; Zhang et al., 2012). Tian et al. (2011) developed a proper orthogonal decomposition (POD)-based ensemble four-dimensional variational assimilation method (PODEn4DVar), which incorporates advantages of both ensemble and variational methods and is suitable for GRACE data assimilation. In this study, a GRACE data assimilation system was developed based on PODEn4DVar and the Community Land Model version 3.5 (CLM3.5, Oleson et al., 2004; 2008), to realize the disaggregation of GRACE data vertically and in time. Its correctness and feasibility were verified by the Observing System Simulation Experiments (OSSEs) at a single point. Assimilation experiments based on GRACE TWSA observations were conducted in China, and preliminary validations were carried out over eight major basins in China.

1 GRACE data assimilation system

In this study, we used the Community Land Model CLM3.5 (Oleson et al., 2004, 2008) as the forecast operator, and PODEn4DVar as the assimilation method in the GRACE data assimilation system.

1.1 Community land model CLM3.5

Spatial land surface heterogeneity in CLM3.5 is represented as a nested subgrid hierarchy, which accounts for land surface characteristic differences at the grid scale, as well as ecological differences among vegetation types and hydraulic and thermal differences among soil types. The subgrid is composed of grid cells, landunits, snow/soil columns, and plant functional types (PFTs). Grid cells may contain different numbers of landunits, including glacier, lake, wetland, urban and vegetated. The vegetated landunit contains several soil/snow columns, and each column is represented by 10 layers for soil and up to five layers for snow. Every soil/snow column contains up to 17 kinds of PFTs, one of

which is for bare ground. This model integrates the advantages of the National Center for Atmospheric Research (NCAR) LSM (Bonan, 1996), the Biosphere-Atmosphere Transfer Scheme (BATS) (Dickinson et al., 1993) and the Institute of Atmospheric Physics, Chinese Academy of Sciences land model (IAP94) (Dai and Zeng, 1997), and has been widely used in research on climate, vegetation ecology and regional hydrological simulation. Based on the earlier version CLM3.0 (Oleson et al., 2004), a new surface dataset was introduced and some modifications were made to the hydrological process in CLM3.5, resulting in more accurate simulation of many hydrological variables and the spatial distribution of vegetation. The modifications to the hydrological process mainly consisted of scaling canopy interception (Lawrence et al., 2007), a simple TOPMODEL-based model for surface and sub-surface runoff (Niu et al., 2005), a simple groundwater model for determining water table depth (Niu et al., 2007b) and a new frozen soil scheme (Niu and Yang, 2006b).

1.2 POD-based ensemble four-dimensional variational assimilation method (PODEn4DVar)

Tian et al. (2008) proposed a hybrid method, referred to as POD4DVar, based on the Monte Carlo method and the POD technique, in which incremental analysis is represented by the POD base with no requirement for the adjoint model. On this basis, Tian et al. (2011) developed the PODEn4DVar method, which integrated the advantages of ensemble methods and variational methods, and can simultaneously assimilate multi-time observations and provide temporal smoothness constraint and flow-dependent background errors. This method obtains the analysis field by minimizing the following incremental format of cost function:

$$J(x') = \frac{1}{2}(x')B^{-1}(x') + \frac{1}{2}[y'(x') - y'_{\text{obs}}]^T R^{-1}[y'(x') - y'_{\text{obs}}], \quad (1)$$

where $x' = x - x_b$, $y' = y'(x') = y(x_b + x') - y(x_b)$, $y'_{\text{obs}} = y_{\text{obs}} - y(x_b)$, $y = H[M_{t_0 \rightarrow t_k}(x)]$. The superscript T represents a transpose, subscript b stands for the background field, obs represents observation, H is the observation operator, M is the forecast model, B is the background error covariance, and R is the observation error covariance.

Define the model perturbation (MP) matrix as $X' = (x'_1, x'_2, \dots, x'_N)$ and the observation perturbation (OP) matrix as $Y' = (y'_1, y'_2, \dots, y'_N)$. Apply the POD transformation to the OP matrix, and the transformed OP samples Φ_y are orthogonal and independent. Then, apply the same

transformation to the MP matrix, and it is evident that the transformed MP samples Φ_x could ensure the orthogonality of their corresponding OP samples. Mark $\Phi_{y,r} = (y'_1, y'_2, \dots, y'_r)$ and $\Phi_{x,r} = (x'_1, x'_2, \dots, x'_r)$, where r is the number of the POD modes, and then the optimal solution can be represented as follows:

$$x'_a = \Phi_{x,r} \beta, \quad (2)$$

where $\beta = (\beta_1, \beta_2, \dots, \beta_r)^T$. Correspondingly, $y'_a = \Phi_{y,r} \beta$ is obtained. By substituting x'_a and y'_a into the cost function, the control variable becomes β instead of x' .

As in the ensemble Kalman filter (EnKF, Evensen, 2004), the background error covariance B is constructed as follows:

$$B = \frac{\Phi_{x,r} \Phi_{x,r}^T}{r-1}. \quad (3)$$

Substitute eqs. (2) and (3) into the cost function. The incremental analysis is obtained by solving the optimal problem. Mark $\tilde{\Phi}_y = [(r-1)I_{r \times r} + \Phi_{y,r}^T R^{-1} \Phi_{y,r}]^{-1} \Phi_{y,r}^T R^{-1}$. The incremental analysis is expressed by

$$x'_a = \Phi_{x,r} \tilde{\Phi}_y y'_{\text{obs}}. \quad (4)$$

Therefore, the final analysis can be calculated from

$$x_a = x_b + x'_a = x_b + \Phi_{x,r} \tilde{\Phi}_y y'_{\text{obs}}. \quad (5)$$

For a more detailed description of PODEn4DVar, refer to Tian et al. (2011).

1.3 GRACE data assimilation system

An observation operator is needed to convert simulated hydrological variables to GRACE-derived TWSA. The observation operator H is defined as follows: for the background vector x_b , which contains the daily model results in the current assimilation window $x_b = (x_{b,1}, x_{b,2}, \dots, x_{b,NT})$, where NT is the number of days in the assimilation window, and $x_{b,k}$ ($k=1, \dots, NT$) contains the simulated SM (solid ice and liquid water), GWS and SWE for the k th day, the simulated TWSA is expressed as

$$y(x_b) = H(x_b) = TWS_{\text{sim}} - TWS_{\text{avg}} = \frac{1}{NT} \sum_{k=1}^{NT} (h(x_{b,k})) - TWS_{\text{avg}}, \quad (6)$$

where TWS_{sim} is the simulated monthly TWS for the current assimilation window, TWS_{avg} is the time-averaged TWS for the study period, and h is the operator to convert daily hydrological variable simulations to TWS.

The core of the GRACE TWS data assimilation system is to transform daily simulations to monthly TWSA using the observation operator and simultaneously update the daily SM, GWS and SWE data. The GRACE data assimilation system includes two steps: first, forecast is done by running CLM3.5 in the current assimilation window to obtain the daily simulations of individual variables; and second, updating is done by carrying out the assimilation calculations and then updating the simulation results during the current window using eqs. (4) and (5). The main processes of the update step are as follows (Figure 1):

(1) Read data, including the GRACE observations and CLM3.5 simulation results in the current assimilation window and the historical results, and then construct the background field vector and the sample matrix.

(2) Calculate the MP matrix X' , the OP matrix Y' and the observation increment y'_{obs} .

(3) Apply the POD transformation to the MP matrix X' , and apply the same transformation to the OP matrix Y' to obtain transformed MP samples Φ_x and OP samples Φ_y .

(4) Calculate the optimal assimilation increment x'_a and the analysis field x_a from eqs. (4) and (5).

(5) Update the CLM3.5 simulations and the initialization file of the current assimilation window by the analysis field.

If the simulation time has not ended, then go back to the forecast step and run CLM3.5 using the updated restart file as the initial condition, and then repeat the update step.

2 Data and experiment design

2.1 Data

This study required near-surface atmospheric forcing data to drive CLM3.5, GRACE-derived TWSA data for data assimilation and evaluation, and the *in situ* soil moisture observa-

tional data for preliminary validation.

Two sets of atmospheric forcing data were used: the Princeton forcing data at three-hourly and $1^\circ \times 1^\circ$ resolution, which combined NCEP–NCAR reanalysis data and observation-based global precipitation, temperature and radiation data, covering the period of 1948–2008 (Sheffield et al., 2006); and the forcing data developed by Tian et al. (2010) (hereafter TIAN), which extended the observation-based atmospheric forcing data from Qian et al. (2006) to 2010, using ERA-interim data (http://data-portal.ecmwf.int/data/d/interim_daily) with six-hourly and $1.5^\circ \times 1.5^\circ$ resolution. The ERA-Interim data assimilated ground-based observation, and therefore their surface fields matched closely with the observation-based reanalysis data, including precipitation and temperature (Simmons et al., 2010).

The GRACE data used in this study were provided by the Tellus product (Wahr et al., 2004; Swenson and Wahr, 2006) processed at the NASA Jet Propulsion Laboratory (JPL). This product was smoothed with a 300 km radius and processed into grid format with monthly and $1^\circ \times 1^\circ$ resolution. This carried data for the 10-year period from April 2002 to May 2011 but, as some monthly data were missing from 2002, 2003 and 2011, the seven years' complete data for 2004–2010 were selected for this study.

The *in situ* soil moisture observation data were obtained from the China Meteorological Data Sharing System. The original data for 778 stations were relative soil moisture content collected every 10 days from agricultural meteorological stations located in farmlands across China. We chose data from 226 stations that were relatively continuous (not more than 20% of the data from March to September were missing), and converted them to monthly volumetric soil moisture in three soil layers of 0–10 cm, 10–20 cm and 70–100 cm. Finally, five years' data for 2004–2008 were used for validation.

2.2 Experimental design

OSSEs at a single point were conducted to verify the correctness and feasibility of the assimilation system developed in this study, and experiments using GRACE observation data were also performed over China. In order to obtain reasonable initial conditions for both sets of experiments, a 100-year CLM3.5 simulation was run using the Princeton atmospheric forcing data, and the final results were used as the initial conditions for all experiments in this study. The OSSEs were conducted on a single point located at (116.5°E, 40.5°N): the CLM3.5 daily simulation results driven by the Princeton forcing data at this point in 2004 were used as the true fields (observations), and the monthly, weekly, two-day and daily TWSA calculated from the true fields were taken as the observations to be assimilated. Then the simulation and assimilation experiments using the four observations with different frequencies were carried out driven by the TIAN atmospheric forcing data of 2004 at this point, and

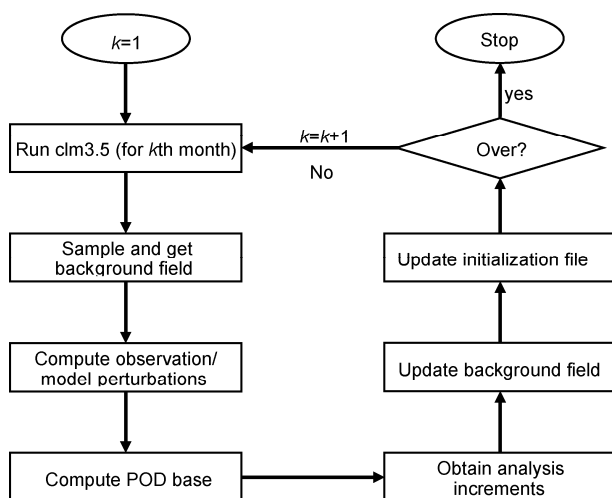


Figure 1 Flow chart of GRACE terrestrial water storage data assimilation system.

the results of the four assimilation experiments were hereafter referred to as Ass_monthly, Ass_weekly, Ass_2day and Ass_daily. Afterwards daily SM and GWS from the true fields were used to evaluate the OSSEs and investigate the sensitivity of the assimilation system to observation frequency.

To further investigate the effect of the assimilation system on the simulations, assimilation experiments based on GRACE-derived TWSA data were carried out with the TIAN atmospheric forcing data over the China region (15°–55°N, 70°–140°E) from 2004 to 2010 with a spatial resolution of 1°×1°, including the CLM3.5 simulation without assimilation (Sim) and simulation using the newly developed assimilation system (Ass). Preliminary validations using in situ soil moisture data were carried out over eight major drainage basins in China (Figure 2).

In both sets of experiments in this study, the ensemble size was set to be 30, and the historical sampling method (Wang et al., 2010) was used: a 30-year run of CLM3.5 using the Princeton forcing data was conducted with the initial conditions described above to obtain daily simulation results; then, in each assimilation window, the sample matrix was generated using the daily results from the time period corresponding to the current assimilation window of every year (including daily SM (10 layers of solid ice and liquid water), GWS and SWE). Since there was only one GRACE observation each month, the assimilation window was set at one month, and the GRACE observation error was set at 20 mm (Zaitchik et al., 2008; Su et al., 2010).

3 Results

3.1 Observing System Simulation Experiments (OSSEs)

The precipitation data for 2004 from the two sets of atmospheric forcing data were compared, and the OSSEs results

were evaluated using the daily observations (Figure 3). Figure 3(a) shows the precipitation time series in 2004 from the Princeton and TIAN atmospheric forcing data, which were different because of their different sources. As a result, the results driven by Princeton forcing data, which were used as observations, also differed from the simulations driven by the TIAN atmospheric forcing data.

The daily TWSA, total column SM (liquid water) and GWS time series are shown in Figure 3(b)–(d), including four assimilation results corresponding to four different observation frequencies. The differences between observed and simulated TWSA were consistent with those from the precipitation series in Figure 3(a), and were especially obvious after July. The four assimilation results from different observation frequencies all improved the simulation of daily TWSA for the whole time period, and the improvements were much more evident after July. The daily variations after assimilation were more consistent with observations. Table 1 gives the correlation coefficients (R) and root mean square errors (RMSE) between simulated, assimilated daily TWSA, total column SM (liquid water), GWS and the observations. Assimilation significantly increased R and decreased RMSE for TWSA. As the observation frequency increased, R increased and RMSE clearly declined, indicating the correctness and feasibility of the assimilation system.

The time series of observed, simulated and assimilated daily SM shown in Figure 3(c) indicate that the model simulation clearly underestimated SM for most of the period; assimilation reduced the degree of underestimation, and the daily variations after assimilation were closer to the observations. As can be seen from Table 1, R and RMSE were both improved by assimilation; as the observation frequency increased, R rose and RMSE gradually fell.

Figure 3(d) shows the time series of the observed, simulated and assimilated daily GWS. The model simulation

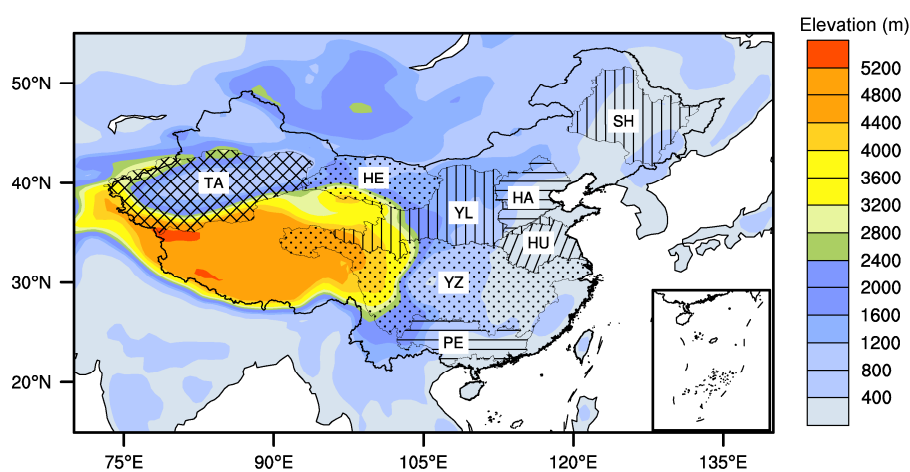


Figure 2 Study area and eight major basins in China: Songhua River Basin (SH), Haihe Basin (HA), Heihe Basin (HE), Tarim Basin (TA), Yellow River Basin (YL), Huaihe Basin (HU), Yangtze River Basin (YZ) and Pearl River Basin (PE).

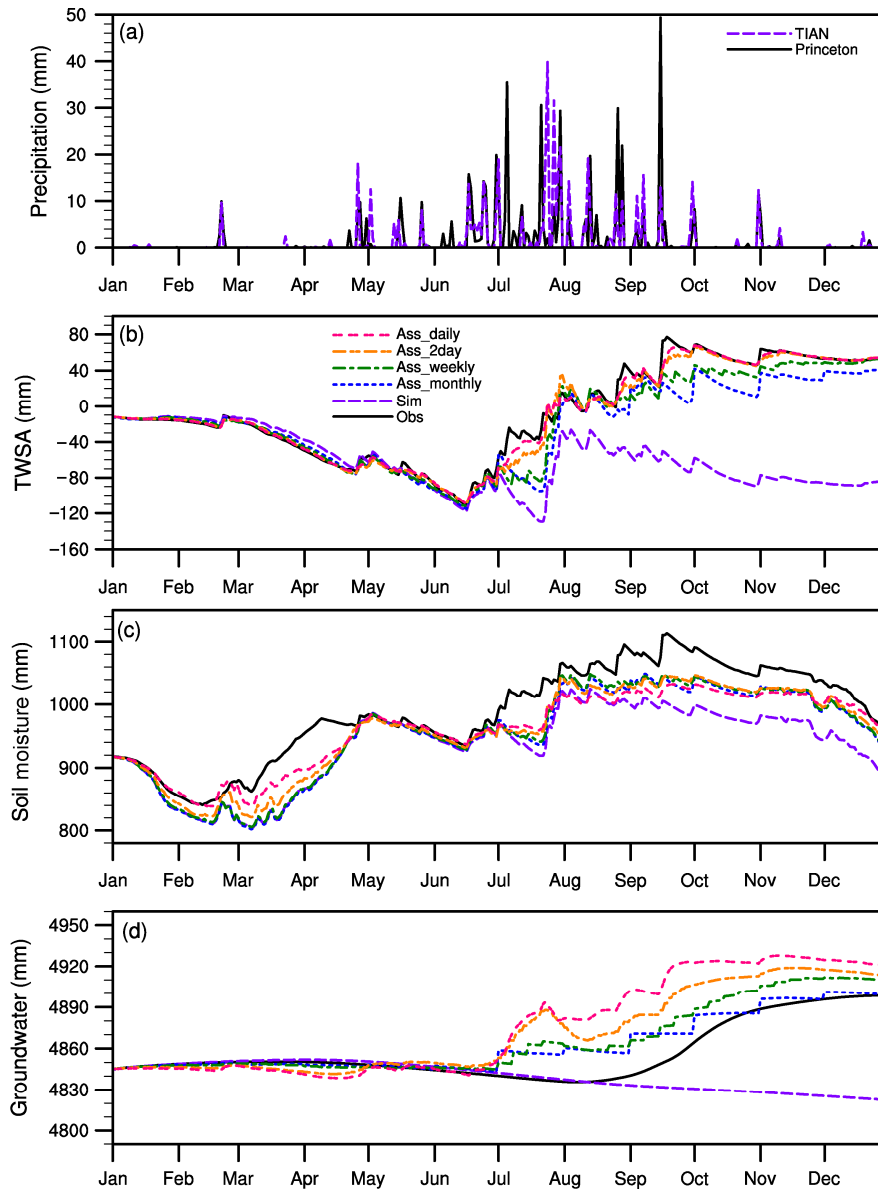


Figure 3 Time series of 2004 precipitation from the Princeton and TIAN atmospheric forcing data used in the OSSEs (a). Daily time series of observations, assimilation and simulation results of OSSEs experiments for TWSA (b), total column SM (liquid water) (c), GWS (d). Ass_monthly, Ass_weekly, Ass_2day and Ass_daily are for the results that assimilated monthly, weekly, two-day and daily observations.

Table 1 Comparison of correlation coefficients and root mean square errors between simulated, assimilated daily TWSA, total SM (liquid water), GWS and observations

		Sim	Ass_monthly	Ass_weekly	Ass_2day	Ass_daily
TWSA	<i>R</i>	-0.0158	0.937	0.960	0.987	0.995
	RMSE	80.901	22.635	16.683	8.777	5.582
Total column soil moisture	<i>R</i>	0.888	0.938	0.942	0.955	0.956
	RMSE	63.689	45.127	42.588	37.513	37.425
Groundwater	<i>R</i>	-0.702	0.896	0.904	0.791	0.718
	RMSE	32.562	10.960	14.307	23.515	31.604

significantly underestimated GWS in the latter stage of the time period; assimilation reduced the extent of underestimation and improved the global variation trend, but with dif-

ferent degrees of overestimation. As can be seen from Table 1, the simulated GWS were negatively correlated with observations, while assimilation greatly improved *R* and re-

duced RMSE, indicating that the daily variations of GWS after assimilation matched more closely with the observation. As the observation frequency increased, R was the largest for weekly observations, and RMSE was the smallest for monthly observations. Obvious changes were found between assimilation windows when assimilating monthly observations. This may be because, when the temporal resolution of TWSA observations was coarse (monthly) and variations of TWSA were visible, differences of observations between two assimilation windows were evident, poor model performances would cause obvious changes between windows. As observation frequency gradually increased, the assimilation window was consequently shorter, and the changes were less obvious, which tends to indicate the reasonableness.

To investigate the influences that data assimilation had on the simulation of daily variations inside one month for individual variables, statistical characteristics were calculated for each month. Compared with the model simulations, R for SM remained almost the same after assimilation, but RMSE fell obviously for most of the months; R for GWS also stayed close to simulations, but RMSE greatly reduced for months when model simulations were poor (results not shown).

Independent data of daily SM and GWS were used to evaluate the OSSEs, indicating that data assimilation could effectively obtain more accurate daily simulations of individual components from monthly TWSA observations, which also compensated for the lack of observations during the validation of assimilation experiments based on GRACE TWSA data. Since the time scale of GRACE observations used in this study was only monthly, the discussion about the sensitivity to observation frequency in the OSSEs did not affect the experiments based on GRACE observations; however, it could be better applied to GRACE data assimilation research in the future.

3.2 Experiments based on GRACE-derived TWSA data

3.2.1 Terrestrial water storage

The GRACE-derived TWSA were converted to absolute TWS via the time-averaged TWS in this study, to compare with simulated and assimilated results and thus evaluate the performance of the assimilation system.

The simulations of TWS over all eight basins in China were greatly improved after assimilation. Figure 4 shows that the TWS simulations of CLM3.5 were unsatisfactory for most basins. The model estimated the seasonal cycle and inter-annual variability of TWS reasonably well, but did not agree well with the observations. The differences in magnitude between simulations and observations were obvious in most basins; also the simulations showed clear upward or downward trends over some of the basins, which were not consistent with the observations. These results showed that,

although CLM3.5 was capable of roughly estimating the TWS over most basins, there was still room for improvement. Compared with model performance, assimilation significantly improved the simulation of TWS in terms of both time variability and magnitude. Aside from the unsatisfactory results for the Songhua River Basin in the final two years of the simulation period, assimilation results matched extremely well with the observations in the other basins. Where the CLM3.5 simulations were not satisfactory, such as the Songhua River Basin, the Heihe Basin in western China, the Tarim Basin and the Yellow River Basin, the improvements due to assimilation were clearly evident, amending the TWS simulations in both time variability and magnitude. Data assimilation also outperformed the model for the Yangtze River and Pearl River basins, where the CLM3.5 simulations were relatively effective, and assimilation results were consistent with the observations. The correlation coefficients and root mean square errors between simulated, assimilated and observed TWS were compared in Figure 5 to further illustrate the assimilation performance. The correlation coefficients for all basins were improved, especially for the Songhua River, Heihe, Tarim and Yellow River basins and all of them approached one, with the exception of the Songhua River Basin. The RMSE all fell to values approaching zero after assimilation, again with the exception of the Songhua River Basin. These results showed that, although the land surface model could roughly simulate the time variations of TWS, clear differences between the simulations and observations were seen, especially for magnitude. The newly developed data assimilation system based on GRACE information significantly improved the estimation of both time variability and magnitude for TWS, which in turn also indicated the correctness and feasibility of the system.

3.2.2 Anomalies of hydrological variables

The purpose of assimilating GRACE-derived TWSA into a land surface model was to merge GRACE information with model simulation in order to disaggregate the column-integrated information vertically and in time, and to globally constrain the hydrological simulations and improve the estimation of individual hydrological variables, for better applications in land surface hydrological research. For this reason, the influences of GRACE data assimilation on the simulation of SM anomalies and GWS anomalies were further evaluated.

Assimilation did not greatly affect the simulation of total column SM anomalies, but improvements were evident in most of the basins. For total SM anomalies in three layers that matched with the *in situ* observations (0–10 cm, 10–20 cm, 70–100 cm), assimilation results were consistent with simulation in half of the basins, but differences were evident for the others. For total column SM, where the water storage was greater than the above three layers, the effect of assimilation was much more obvious, and adjust-

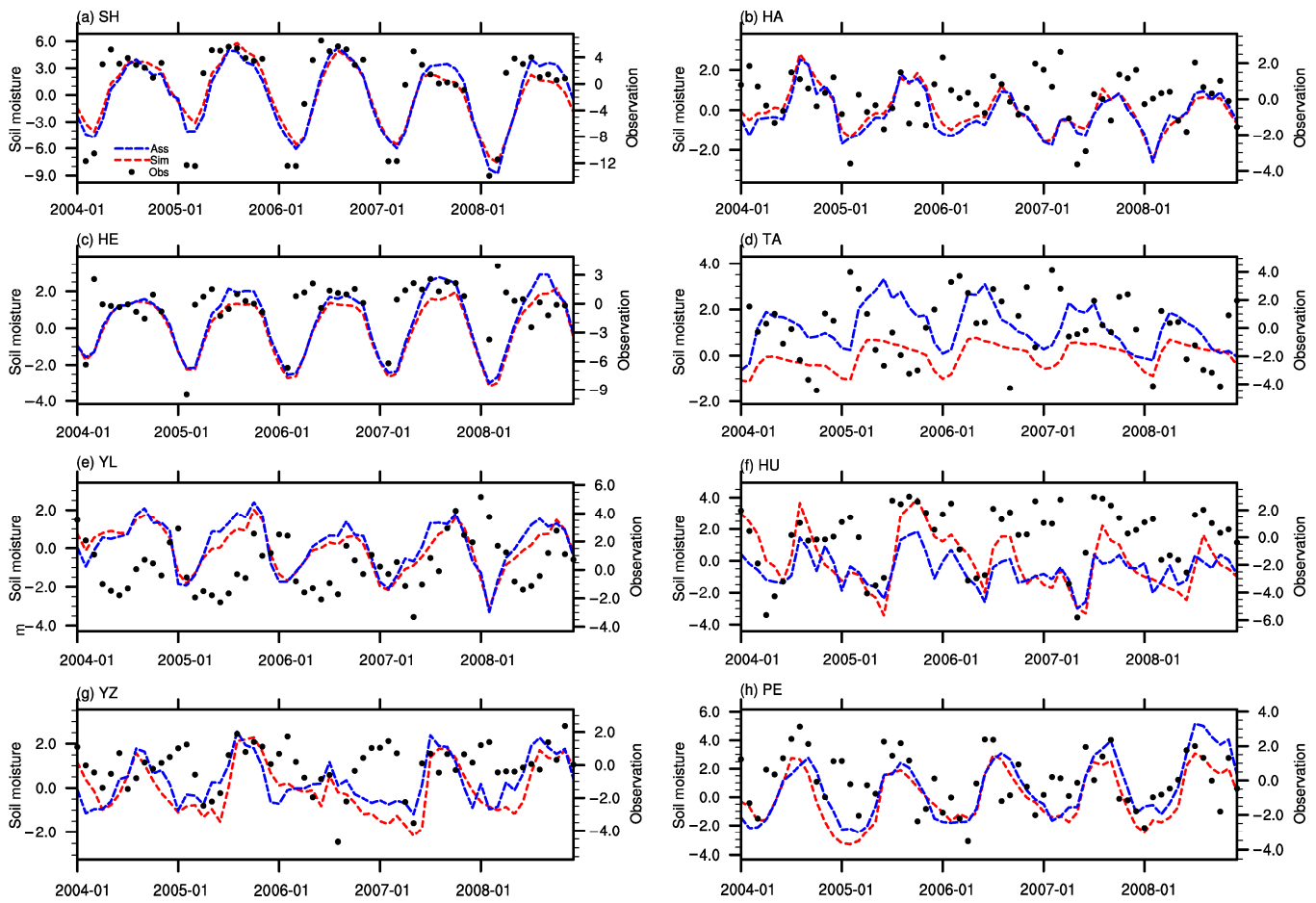


Figure 4 Daily TWS series based on GRACE observations. Black dots: absolute TWS converted from GRACE TWSA observations; red lines: simulation results; blue lines: assimilation results.

ments were evident for most of the basins after assimilation (results not shown). Constrained by *in situ* SM observations, the total column SM anomalies from simulation and assimilation were compared with the total SM anomalies observed at the above three layers (Figure 6). The time variations of the simulated total column SM anomalies remained almost identical to the observed three-layer anomalies for most of the basins, but were negatively correlated in some basins. For most of the basins, assimilation results were clearly different from the simulations and improved the correlation coefficients to different degrees, reflecting that GRACE data assimilation could adjust and improve the simulations of SM.

The improvements that GRACE data assimilation had on the simulations of GWS were much more obvious than SM. Figure 7 shows the time series of simulated and assimilated GWS anomalies together with GRACE-derived TWSA from 2004 to 2010. The figure shows that the land surface model did not simulate the GWS time variations correctly, and even negative correlations were found for the Heihe and Huaihe Basins. Data assimilation greatly improved the simulation of time variations for GWS, and the assimilation results matched much better with the GRACE-derived

TWSA. The correlation coefficients shown in Table 2 also greatly increased for six of the basins after assimilation.

The results for water table depth (WTD) were similar to those for GWS. The model produced a more accurate simulation of WTD than that of GWS, but improvements were still needed in some basins. After assimilation, the WTD anomalies agreed well with the GRACE-derived TWSA, and the correlation coefficients for all the basins were increased to different extents.

3.2.3 Southwest drought

Southwest China is an important agricultural production region, and seasonal droughts are the main agro-meteorological disasters in this area. A very rare and serious drought, which lasted from September 2009 to April 2010, affected Guangxi, Yunnan, Guizhou, Chongqing and Sichuan in Southwest China, and the local agricultural production and social economy suffered a great loss. The GRACE-derived TWSA captured this drought well; as Figure 8 shows, the GRACE observations detected that most areas in the region were losing water, with two negative anomaly centers located at the junction of Yunnan, Sichuan and Tibet and the junction of Yunnan and Guangxi. How-

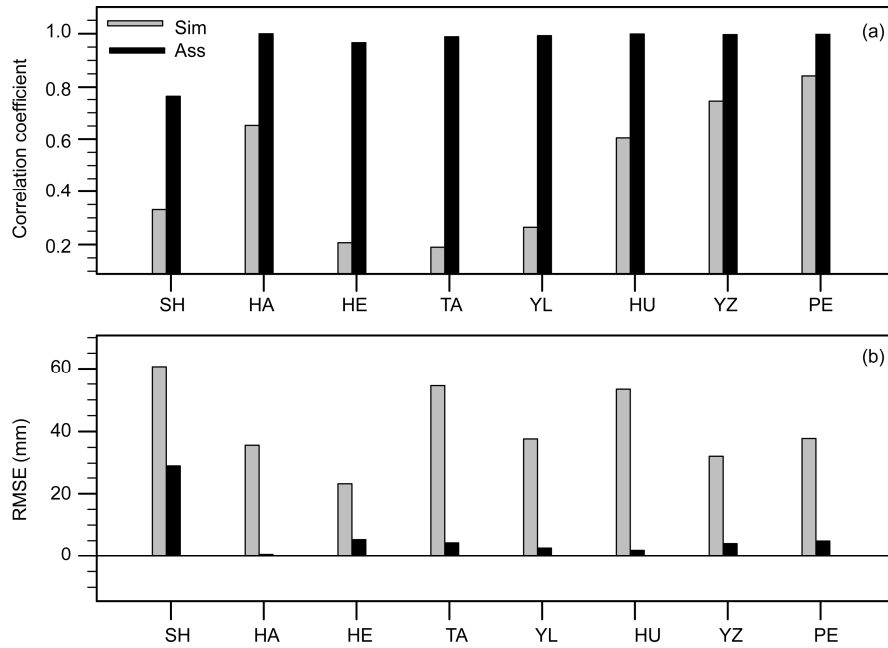


Figure 5 Comparison of correlation coefficients and root mean square errors for assimilated and simulated TWS and GRACE-derived TWS. Gray: simulation results; black: assimilation results.

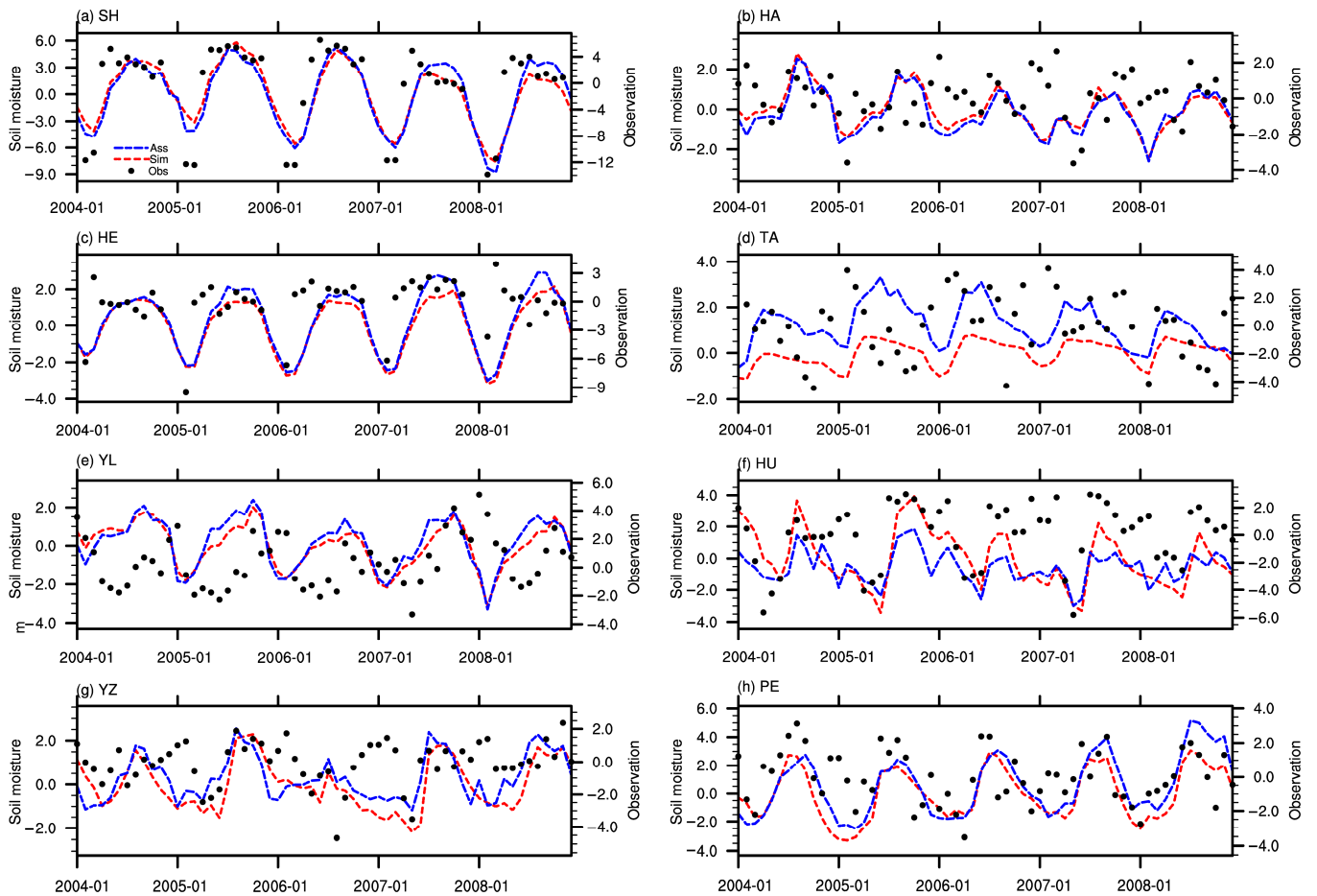


Figure 6 Monthly time series of simulated and assimilated SM anomalies, together with *in situ* observations for 2004–2008 ($10^{-2} \text{ m}^3 \text{ m}^{-3}$). Black dots: *in situ* observations; red lines: simulation results; blue lines: assimilation results. Simulation and assimilation results for total column SM anomalies on left-hand vertical axis; observed SM anomalies for three layers (0–10 cm, 10–20 cm, 70–100 cm) on right-hand vertical axis.

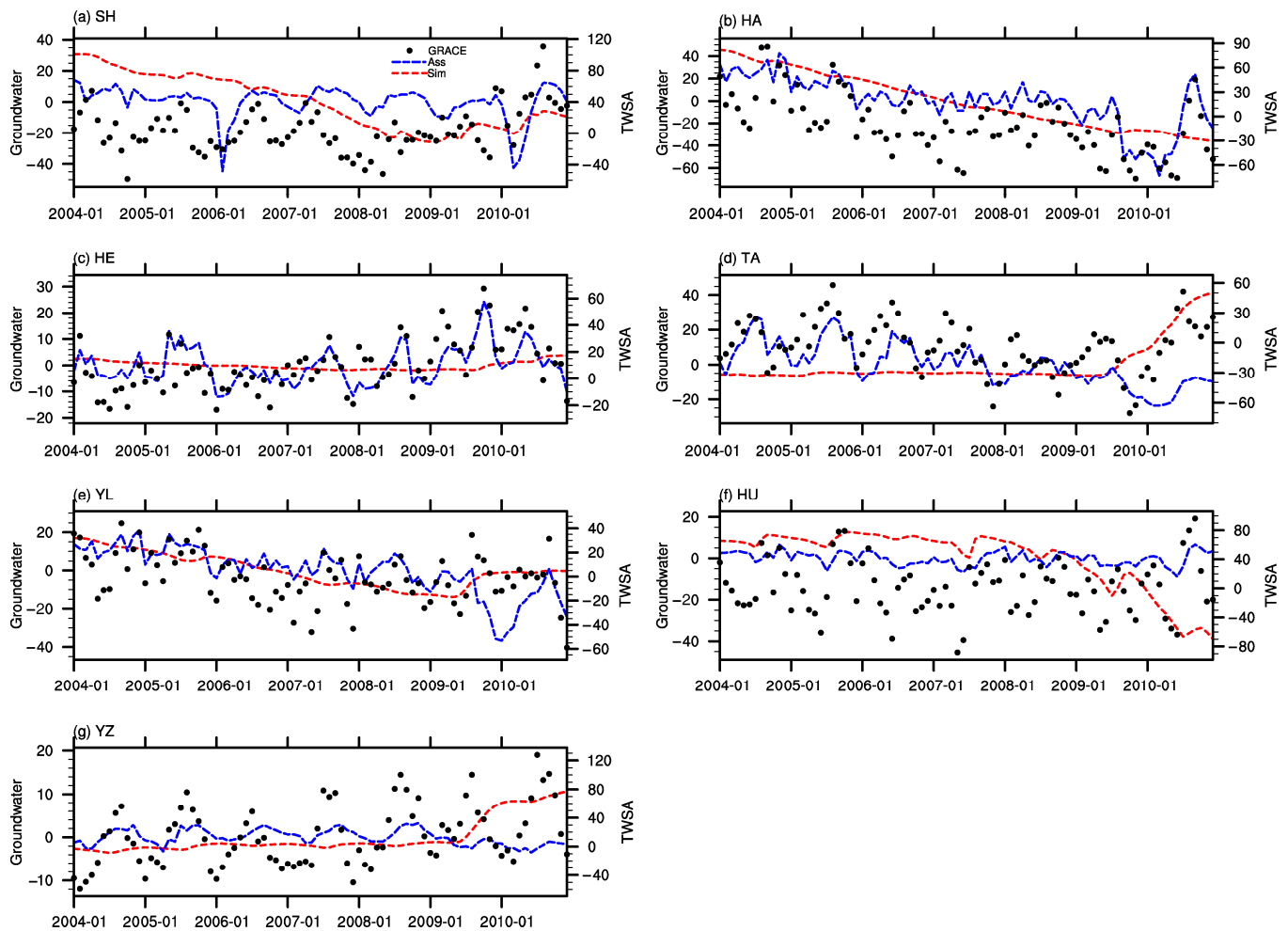


Figure 7 Monthly time series of simulated and assimilated GWS anomalies (mm) (left-hand vertical axis) and GRACE-derived TWSA (mm) (right-hand vertical axis) from 2004 to 2010. Black dots: GRACE-derived TWSA; red lines: simulation results; blue lines: assimilation results.

Table 2 Comparison of correlation coefficients between assimilated, simulated GWS and WTD anomalies and GRACE-derived TWSA for the eight basins^{a)}

Basins		SH	HA	HE	TA	YL	HU	YZ	PE
Groundwater anomaly	Ass	0.165	0.811	0.756	0.490	0.498	0.553	0.178	—
	Sim	0.044	0.588	-0.116	0.195	0.384	-0.008	0.257	—
Water table depth anomaly	Ass	0.331	0.682	0.336	0.311	0.363	0.641	0.891	0.907
	Sim	0.328	0.588	-0.092	0.253	0.223	0.520	0.810	0.861

a) For the abbreviations of basin names see the legends to Figure 2.

ever, the land surface model simulations did not present a similar pattern, with positive anomalies in Sichuan, Chongqing, Yunnan and most of Guangxi, and negative anomalies only in Guizhou, all of which were inconsistent with the facts. Data assimilation greatly outperformed the model. Although the magnitudes after assimilation differed from the observations, the spatial distribution pattern was approximately the same as GRACE with the two negative anomaly centers, which agreed very well with observations. As we can tell from the differences between simulation and assimilation results, the model simulations were too wet for Southwest China from the fall of 2009 to the spring of 2010,

while data assimilation had very significant improvements.

This severe and comprehensive drought involved meteorological, hydrological, agricultural and social economic aspects (Yin and Li, 2013). Since the essence of an agricultural drought is that the soil moisture is too low to meet the water demand of the vegetation, this aspect should be reflected by soil moisture anomalies for this period. Figure 9 shows the simulated and assimilated spatial distribution of the total column soil water storage anomalies for the drought period. The model simulation showed positive anomalies (i.e., increased soil moisture) in most areas, while negative anomalies were seen only in some parts of Guang-

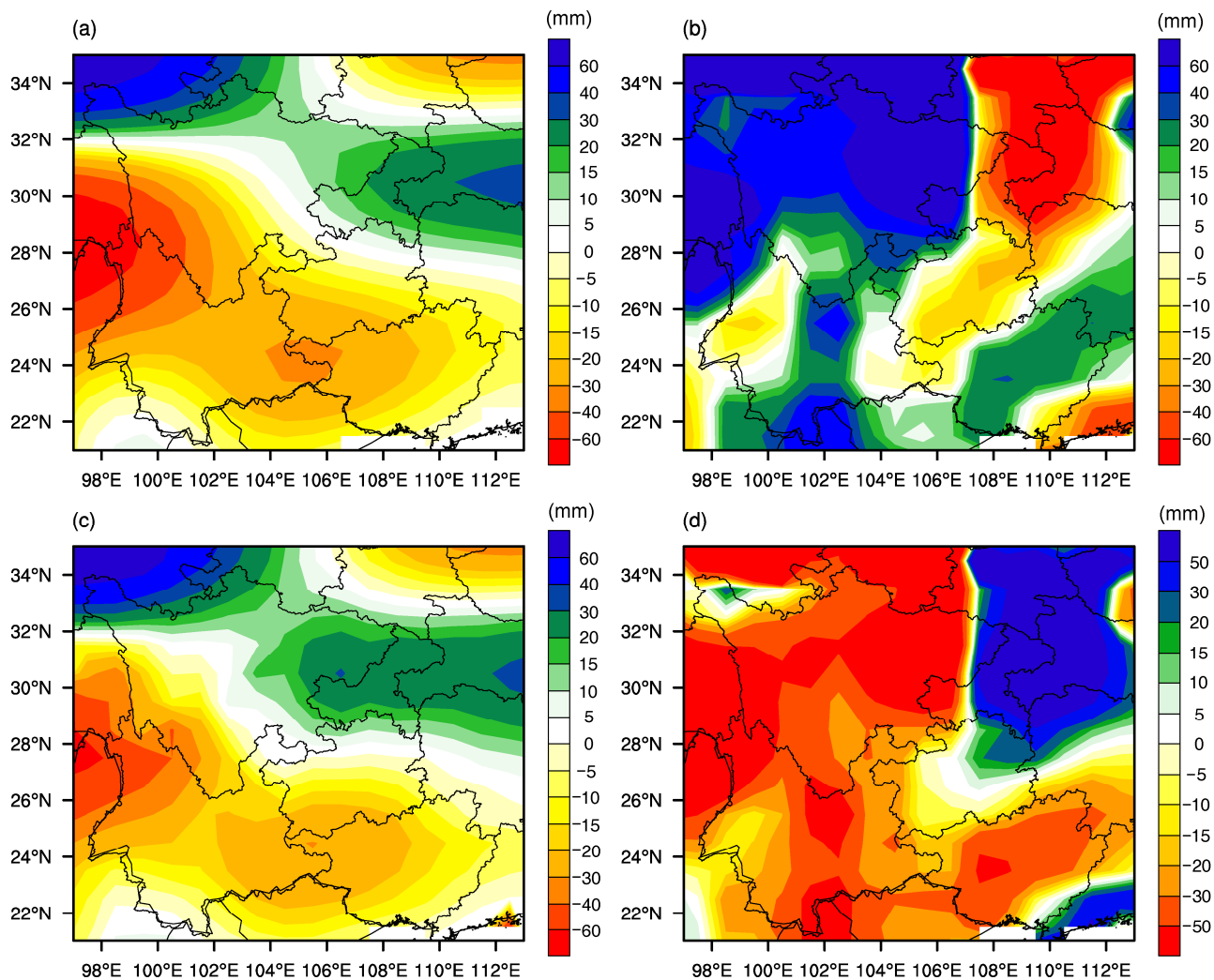


Figure 8 Spatial distribution of TWSA in Southwest China, averaged for the period of September 2009–April 2010. (a) GRACE observations; (b) simulation results; (c) assimilation results; (d) difference between assimilation and simulation results.

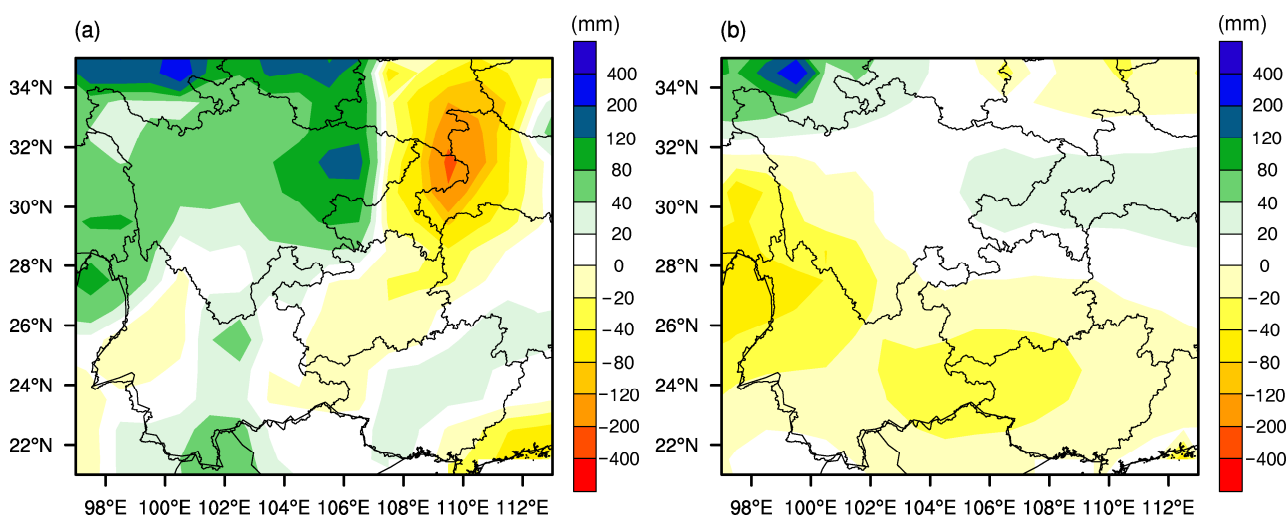


Figure 9 Spatial distribution of SM anomalies in Southwest China averaged for September 2009–April 2010. (a) Simulation results; (b) assimilation results.

xi and Yunnan; that is, drought conditions were not indicated. Data assimilation performed much better than model simulation. Most regions of the five provinces were losing water after assimilation, with two negative centers, reflecting the true spatial range of the drought.

The spatial distribution and negative centers of soil water storage anomalies in Figure 9 agreed well with GRACE observations in Figure 8, and adjustments in the magnitude of the soil water content were evident, indicating the capability of data assimilation to effectively disaggregate the GRACE information vertically and improve the simulation of individual hydrological variables. These evaluations, though simple and preliminary in nature, were nevertheless indicative of the potential of the GRACE data assimilation system for drought monitoring research.

4 Discussion and summary

A GRACE data assimilation system was developed in this study, which assimilated the GRACE-derived TWSA information into the Community Land Model CLM3.5 through the ensemble four-dimensional variational assimilation method PODEn4DVar, in order to disaggregate the monthly and column-integrated GRACE information both vertically and in time, and convert the integrated information into changes of individual variables (including SM, GWS and SWE in this study). Single-point OSSEs were designed to verify the feasibility of the system, while assimilation experiments based on GRACE observations were carried out in China, and preliminary evaluations were conducted over eight major basins and the southwestern areas.

The results of the OSSEs showed that GRACE data assimilation could improve the simulation of land surface hydrological variables, indicating the feasibility of the assimilation system. Correlation coefficients and root mean square errors between assimilation results and daily observations were improved significantly, demonstrating that data assimilation could produce more accurate daily variations of individual variables from the monthly and column-integrated TWSA observations. Experiments that assimilated observations of different frequencies showed that, as the observation frequency increased, data assimilation performed better for SM with relatively rapid variations, but similar results did not hold for GWS with relatively slow variations.

Assimilation experiments based on GRACE-derived TWSA observations and preliminary validations were conducted over eight major basins in China, to explore the effect that GRACE data assimilation had on the simulations of hydrological variables. It was found that data assimilation significantly improved TWS simulations, with results agreed very well with GRACE observations, and correlation coefficients and root mean square errors greatly improved as well. Data assimilation did not have a marked effect on

the simulations of SM anomalies, and yet improved the correlation coefficients for most of the basins. The influences of data assimilation on the simulation of GWS anomalies and WTD anomalies were much more visible. Correlation coefficients between GWS and WTD anomalies after assimilation and the GRACE-derived TWSA observations were greatly improved for almost all the basins. Data assimilation also captured the 2009–2010 drought event that took place in Southwest China in terms of TWSA and SM anomalies. All of these results illustrated that the GRACE data assimilation system had a considerable potential for improving simulations of hydrological variables and for applications in drought monitoring.

The evaluations of the experiments based on GRACE-derived TWSA data were conducted at the scale of basins; however, the variation characteristics of SM and GWS in upstream regions of the larger basins may differ considerably from that downstream. Therefore it may be neither representative nor significant to take average values over the whole basin. Evaluations over smaller regions that are determined by climate may reflect the impacts of data assimilation much better and further illustrated its effects for different climate regions, so as to better apply in water cycle and drought monitoring. This still needs further discussion. Notably, while GRACE-derived TWSA observations integrate change information from any depth, only GWS, SM and SWE were considered in this study, and the land surface model used can only depict water storage changes in unconfined aquifer; meanwhile, the GRACE observations are able to detect the influences of human activities on GWS, which are not considered in the model. The discrepancies between observation and model not only can promote the further development of the GRACE data assimilation, but also can bring new ideas for the future development of land surface models.

Only preliminary and simple validations were carried out in this study. The fact that assimilating SM and GWS can have destabilizing impacts on other model processes suggests that the effects on the simulations of runoff and evaporation need to be investigated, as well as further applications in drought monitoring. The forecast operator used in this study was the Community Land Model CML version 3.5. It has subsequently been developed to version 4.5 and incorporated into the Community Earth System Model as the land module, and many improvements have been made to the hydrological process. Therefore, the forecast operator needs to be updated, so that to enhance the accuracy of the data assimilation system. The spatial resolution of GRACE observations is very coarse, and disaggregation in the horizontal direction has not yet been achieved in this study. In future work it is intended to conduct the GRACE data assimilation research at a higher spatial resolution to disaggregate the GRACE information horizontally, and high-resolution datasets of TWS and other hydrological variables will be generated for better applications in land surface hydrological research and drought monitoring.

We are grateful Prof. Xin Li and the anonymous reviewer for their valuable comments and suggestions. This study was supported by the National Natural Science Foundation of China (Grant Nos. 41075062, 91125016) and the National Basic Research Program of China (Grants Nos. 2010CB951001, 2010CB428403).

- Bonan G B. 1996. Land Surface Model (LSM version 1.0) for ecological, hydrological, and atmospheric studies: Technical description and user's guide. NCAR Tech Note 417+STR
- Chen J L, Wilson C R, Tapley B D. 2011. Interannual variability of Greenland ice losses from satellite gravimetry. *J Geophys Res*, 116: B07406
- Chen J L, Wilson C R, Tapley B D, et al. 2010. Recent La Plata basin drought conditions observed by satellite gravimetry. *J Geophys Res*, 115: D22108
- Chen J L, Wilson C R, Tapley B D, et al. 2009b. 2005 drought event in the Amazon River basin as measured by GRACE and estimated by climate models. *J Geophys Res*, 114: B05404
- Chen J L, Wilson C R, Blankenship D, et al. 2009a. Accelerated Antarctic ice loss from satellite gravity measurements. *Nat Geosci*, 2: 859–862
- Dai Y J, Zeng Q C. 1997. A land surface model (IAP94) for climate studies part I: Formulation and validation in off-line experiments. *Adv Atmos Sci*, 14: 433–460
- Dickinson R, Henderson-Sellers A, Kennedy P. 1993. Biosphere-Atmosphere Transfer Scheme (BATS) Version 1 as Coupled to the NCAR Community Climate Model. NCAR Tech Note NCAR/TN387+STR
- Evensen G. 2004. Sampling strategies and square root analysis schemes for the EnKF. *Ocean Dyn*, 53: 539–560
- Feng W, Zhong M, Lemoine J M, et al. 2013. Evaluation of groundwater depletion in North China using the Gravity Recovery and Climate Experiment (GRACE) data and ground-based measurements. *Water Resour Res*, 49: 2110–2118
- Forman B A, Reichle R H, Rodell M. 2012. Assimilation of terrestrial water storage from GRACE in a snow-dominated basin. *Water Resour Res*, 48: W01507
- Grippa M, Kergoat L, Frappart F, et al. 2011. Land water storage variability over West Africa estimated by Gravity Recovery and Climate Experiment (GRACE) and land surface models. *Water Resour Res*, 47: W05549
- Houborg R, Rodell M, Li B, et al. 2012. Drought indicators based on model-assimilated Gravity Recovery and Climate Experiment (GRACE) terrestrial water storage observations. *Water Resour Res*, 48: W07525
- Hu X G, Chen J L, Zhou Y H, et al. 2006. Seasonal water storage change of the Yangtze River basin detected by GRACE. *Sci China Ser D-Earth Sci*, 49: 483–491
- Konikow L F. 2011. Contribution of global groundwater depletion since 1900 to sea-level rise. *Geophys Res Lett*, 38: L17401
- Lawrence D M, Thornton, and Oleson K W, et al. 2007. The partitioning of evapotranspiration into transpiration, soil evaporation, and canopy evaporation in a GCM: Impacts on land-atmosphere interaction. *J Hydrometeorol*, 8: 862–880
- Li B, Rodell M, Zaitchik B F, et al. 2012. Assimilation of GRACE terrestrial water storage into a land surface model: Evaluation and potential value for drought monitoring in western and central Europe. *J Hydrol*, 446: 103–115
- Li X, Huang C L, Che T, et al. 2007. Development of a Chinese land data assimilation system: Its progress and prospects. *Prog Nat Sci*, 17: 881–892
- Llovel W, Becker M, Cazenave A, et al. 2011. Terrestrial waters and sea level variations on interannual time scale. *Glob Planet Change*, 75: 76–82
- Lo M H, Famiglietti J S, Yeh P J-F, et al. 2010. Improving parameter estimation and water table depth simulation in a land surface model using GRACE water storage and estimated base flow data. *Water Resour Res*, 46: W05517
- Niu G Y, Yang Z L. 2006a. Assessing a land surface model's improvements with GRACE estimates. *Geophys Res Lett*, 33: L07401
- Niu G Y, Yang Z L. 2006b. Effects of frozen soil on snowmelt runoff and soil water storage at a continental scale. *J Hydrometeorol*, 7: 937–952
- Niu G Y, Seo K W, Yang Z L, et al. 2007a. Retrieving snow mass from GRACE terrestrial water storage change with a land surface model. *Geophys Res Lett*, 34: L15704
- Niu G Y, Yang Z L, Dickinson R E, et al. 2005. A simple TOPMODEL-based runoff parameterization (SIMTOP) for use in global climate models. *J Geophys Res*, 110: D21106
- Niu G Y, Yang Z L, Dickinson R E, et al. 2007b. Development of a simple groundwater model for use in climate models and evaluation with Gravity Recovery and Climate Experiment data. *J Geophys Res*, 112: D07103
- Oleson K W, Coauthors. 2008. Improvements to the community land model and their impact on the hydrological cycle. *J Geophys Res*, 113: G01021
- Oleson K W, Dai Y J, Bonan G, et al. 2004. Technical description of the Community Land Model (CLM). NCAR Tech Note NCAR/TN461+STR
- Qian T T, Dai A G, Trenberth K E, et al. 2006. Simulation of global land surface conditions from 1948 to 2004. Part I: Forcing data and evaluations. *J Hydrometeorol*, 7: 953–975
- Qiu C J, Shao A M, Xu Q, et al. 2007. Fitting model fields to observations by using singular value decomposition: An ensemble-based 4DVar approach. *J Geophys Res*, 112: D11105
- Rodell M, Chen J L, Kato H, et al. 2007. Estimating ground water storage changes in the Mississippi River basin (USA) using GRACE. *Hydrogeol J*, 15: 159–166
- Rodell M, Famiglietti J S, Chen J L, et al. 2004. Basin scale estimates of evapotranspiration using GRACE and other observations. *Geophys Res Lett*, 31: L20504
- Rowlands D D, Luthcke S B, Klosko S M, et al. 2005. Resolving mass flux at high spatial and temporal resolution using GRACE intersatellite measurements. *Geophys Res Lett*, 32: L04310
- Sheffield J, Ferguson C R, Troy T J, et al. 2009. Closing the terrestrial water budget from satellite remote sensing. *Geophys Res Lett*, 36: L07403
- Sheffield J, Goteti G, Wood E F. 2006. Development of a 50-year high-resolution global dataset of meteorological forcings for land surface modeling. *J Clim*, 19: 3088–3111
- Simmons A J, Willett K M, Jones P D, et al. 2010. Low-frequency variations in surface atmospheric humidity, temperature, and precipitation: Inferences from reanalyses and monthly gridded observational data sets. *J Geophys Res*, 115: D01110
- Su H, Yang Z L, Dickinson R E, et al. 2010. Multisensor snow data assimilation at the continental scale: The value of gravity recovery and climate experiment terrestrial water storage information. *J Geophys Res*, 115: D10104
- Su X L, Ping J S, Ye Q X. 2012. Terrestrial water storage changes of North China revealed from GRACE gravity measurements. *Sci China Earth Sci*, 42: 917–922
- Sun W K. 2002. Satellite in low orbit (CHAMP, GRACE, GOCE) and high precision earth gravity field: the latest progress of satellite gravity geodesy and its great influence on geoscience. *J Geod Geodyn*, 22: 92–100
- Swenson S, Wahr J. 2006. Post-processing removal of correlated errors in GRACE data. *Geophys Res Lett*, 33: L08402
- Syed T H, Famiglietti J S, Chambers D. 2009. GRACE-based estimates of terrestrial freshwater discharge from basin to continental scales. *J Hydrometeorol*, 10: 22–40
- Syed T H, Famiglietti J S, Rodell M, et al. 2008. Analysis of terrestrial water storage changes from GRACE and GLDAS. *Water Resour Res*, 44: W02433
- Tapley B, Bettapur S, Ries J, et al. 2004a. GRACE measurements of mass variability in the Earth system. *Sci*, 305: 503–505
- Tapley B, Bettapur S, Watkins M, et al. 2004b. The Gravity Recovery and Climate Experiment: Mission overview and first results. *Geophys Res Lett*, 31: L09607
- Tian X J, Xie Z H, Dai A G. 2008. An ensemble-based explicit four-dimensional variational assimilation method. *J Geophys Res*, 113: D21124
- Tian X J, Xie Z H, Sun Q. 2011. A POD-based ensemble four-dimensional

- variational assimilation method. *Tellus Ser A-Dyn Meteorol Oceanol*, 63: 805–816
- Tian X J, Xie Z H, Dai A G, et al. 2010. A microwave land data assimilation system: Scheme and preliminary evaluation over China. *J Geophys Res*, 115: D21113
- Troy T J, Sheffield J, Wood E F. 2011. Estimation of the terrestrial water budget over northern Eurasia through the use of multiple data sources. *J Clim*, 24: 3272–3293
- Wahr J, Swenson S, Zlotnicki V, et al. 2004. Time variable gravity from GRACE: First results. *Geophys Res Lett*, 31: L11501
- Wang B, Liu J J, Wang S D, et al. 2010. An economical approach to four-dimensional variational data assimilation. *Adv Atmos Sci*, 27: 715–727
- Wang T, Mu M. 2008. A REM adjoint system and its data assimilation experiments of 4D-VAR. *Acta Meteorol Sin*, 66: 955–967
- Wouters B, Riva R E M, Lavallée D A, et al. 2011. Seasonal variations in sea level induced by continental water mass: First results from GRACE. *Geophys Res Lett*, 38: L03303
- Xu M, Ye B S, Zhao Q D. 2013. Temporal and spatial pattern of water storage changes over the Yangtz river basin during 2002–2010 based on GRACE satellite data. *Prog Geogr*, 1: 008
- Yang K, Watanabe T, Koike T, et al. 2007. Auto-calibration system developed to assimilate AMSR-E data into a land surface model for estimating soil moisture and the surface energy budget. *J Meteorol Soc Jpn*, 85: 229–242
- Yeh P J F, Swenson S C, Famiglietti J S, et al. 2006. Remote sensing of groundwater storage changes in Illinois using the Gravity Recovery and Climate Experiment (GRACE). *Water Resour Res*, 42: W12203
- Yin H, Li Y H. 2013. Summary of advance on drought study in Southwest China. *J Arid Meteorol*, 31: 182–193
- Zaitchik B F, Rodell M, Reichle R H. 2008. Assimilation of GRACE terrestrial water storage data into a land surface model: Results for the Mississippi River basin. *J Hydrometeorol*, 9: 535–548
- Zhang S L, Shi J C, Dou Y J. 2012. A soil moisture assimilation scheme based on the microwave Land Emissivity Model and the Community Land Model. *Int J Remote Sens*, 33: 2770–2797
- Zhong M, Duan J B, Xu H Z, et al. 2009. Trend of China land water storage redistribution at medi- and large-spatial scales in recent five years by satellite gravity observations. *Chin Sci Bull*, 54: 816–821.
- Zhu J, Zhou G Q, Yan C X, et al. 2007. The design and preliminary application of a three-dimensional variational ocean data assimilation system. *Sci China Ser D-Earth Sci*, 37: 261–271